Available online at www.sciencedirect.com
ScienceDirect
Optik 121 (2010) 1257–1262
Optik Optics
www.elsevier.de/ijleo

A theoretical study of double-pass thulium-doped fiber amplifiers

S.D. Emami[a,*], S.W. Harun[a], F. Abd-Rahman[d], H.A. Abdul-Rashid[b], S.A. Daud[b], Z.A. Ghani[c], H. Ahmad[a]

[a]*Photonics Research Center, University of Malaya, 50603 Kuala Lumpur, Malaysia*
[b]*Faculty of Engineering, Multimedia University, 63100 Cyberjaya, Malaysia*
[c]*Faculty of Applied Science, University Technology MARA, 40450 Shah Alam, Malaysia*
[d]*Faculty of Engineering and Science, Universiti Tunku Abdul Rahman 53300 Setapak, Malaysia*

Received 1 September 2008; accepted 12 January 2009

Abstract

An efficient fluoride-based thulium-doped fiber amplifier (TDFA) is theoretically demonstrated using a double-pass scheme. A reflector is incorporated in the double-pass TDFA to allow double propagation of the test signal in the gain medium and thus improve the gain of the TDFA. The small signal gain improvement of more than 15 dB is obtained in the 1465 nm region. A gain as high as 42 dB is obtained in this region with 300 mW of 1050 nm pump using 20 m of thulium-doped fiber. However, a noise figure penalty of approximately 1 dB is also obtained in this wavelength region. Differential equations are solved using the Runge–Kutta method in the theoretical analysis. The theoretical result is in agreement with the experimental result.

Keywords: Thulium-doped fiber amplifier; S-band amplifier; Double pass

1. Introduction

Due to the tremendous increase in communication traffic in recent years, more and more efforts in research have been directed towards developing highly efficient broad-band fiber amplifiers that will fully exploit the low-loss band of silica fibers in the 1450–1630 nm range, which has a loss of only 0.25 dB/km in order to increase the transmission capacity of wavelength-division multiplexing (WDM) networks [1,2]. These broad-band amplifiers must be able to amplify the new short wavelength band (S-band) in addition to the existing C- and L-bands. Thulium-doped fluoride fiber amplifiers (TDFFAs) are a promising candidate for the S-band amplification because the amplification bandwidth of the TDFA is centered at 1470 nm [3], which falls within the S-band. However, its power conversion efficiency and its spectral gain characteristics are crucial issues that need to be addressed [4–6]. Several studies dealing with gain enhancement have been reported [7–10], leading to an improvement of pumping efficiency through an up-conversion pumping scheme.

In this paper, an efficient TDFFA is demonstrated theoretically using a double-pass scheme. The thulium-doped fluoride fiber is pumped by a 1050 nm laser diode using a forward pumping scheme. A reflector is used at the output end of the amplifier to allow a double propagation of the forward amplified spontaneous emission (ASE) and the optical signal in the thulium-doped fiber. Differential equations involved in the theoretical analysis are solved using the Runge–Kutta method [11,12].

*Corresponding author.
E-mail address: S.D.Emami@gmail.com (S.D. Emami).

0030-4026/$ - see front matter © 2009 Elsevier GmbH. All rights reserved.
doi:10.1016/j.ijleo.2009.01.017

2. Configuration and modeling of the TDFA

Fig. 1 shows the configuration of the double-pass TDFA, which consists of a fluoride-based TDF, a WDM coupler, a pump laser, an optical circulator and a reflector. The TDF used is 20 m long and has a Tm ion concentration of 2000 ppm. The pump light and the input signal are combined using a WDM coupler. A 1050 nm laser diode is used as the pump. Both the forward ASE and the signal are reflected back into the system by a reflector. An optical circulator is then used to route the output and to prevent the backscattered light from entering the transmitter.

Fig. 2 shows the energy level diagram of trivalent thulium ion in fluoride glass. Figs. 2 (a) and (b) show the absorption and emission transitions, respectively, in the TDFA with 1050 nm pump. As shown in the figure, the main transition used for S-band amplification is between $^3H_4$ and $^3F_4$ levels, which emit photons at 1460 nm region. This amplification is made possible by an up-conversion pumping method, which forms a population inversion between $^3H_4$ and $^3F_4$ levels. When the TDF is pumped with 1050 nm laser, the ground-state ions in the $^3H_6$ energy level can be excited to the $^3H_5$ energy level and then relaxed to the $^3F_4$ energy level by non-radiative decay. The $^3F_4$ energy level ions are then re-excited to the $^3F_2$ energy level and experience non-radiative decay to the $^3H_4$ energy level via excited-state absorption. The 1050 nm pump alone can provide both the ground-state and excited-state absorptions.

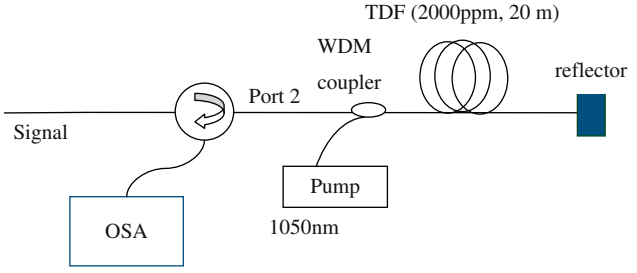

Fig. 1. Configuration of the double-pass TDFA.

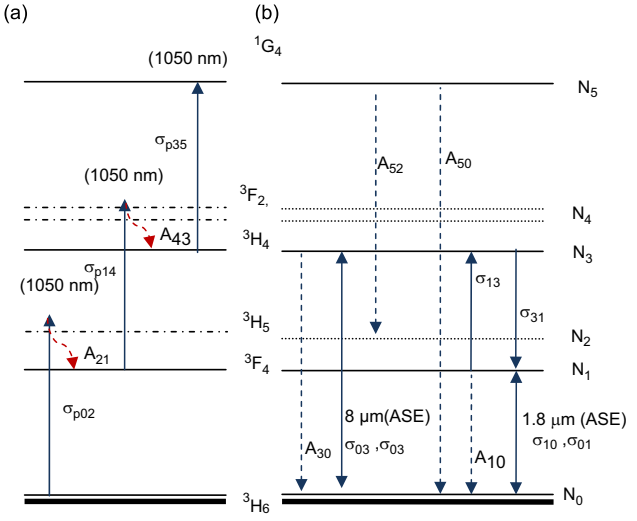

Fig. 2. Energy level diagram of thulium ion.

The difference between the $^3F_2$ and $^3F_3$ energy levels is very small and therefore they can be treated as one level for simplicity [13]. We substitute N_0, N_1, N_2, N_3, N_4 and N_5 variables for ion populations of $^3H_6$, $^3F_4$, $^3H_5$, $^3H_4$, $^3F_2$ and $^1G_2$ respectively. According to Fig. 2, the rate equations can be established as follows:

$$\frac{dN_0}{dt} = -(W_{p02} + W_{18a} + W_{8a})N_0 + (A_{10} + W_{18e})N_1 + (A_{30} + W_{8e})N_3 + A_{50}N_5 \quad (1)$$

$$\frac{dN_1}{dt} = (W_{18a})N_0 - (A_{10} + W_{p14} + W_{sa} + W_{18e})N_1 + (A_{20})N_2 + (W_{se})N_3 \quad (2)$$

$$\frac{dN_2}{dt} = (W_{p02})N_0 - (A_{21}^{nr})N_2 + (W_{52})N_5 \quad (3)$$

$$\frac{dN_3}{dt} = (W_{8a})N_0 + (W_{sa})N_1 - (A_{30} + W_{p35} + W_{se} + W_{8a})N_3 + (A_{43})N_4 \quad (4)$$

$$\frac{dN_4}{dt} = (W_{p14})N_1 - (A_{43}^{nr})N_4 \quad (5)$$

$$\frac{dN_5}{dt} = (W_{p35})N_3 - (A_{50} + A_{52})N_5 \quad (6)$$

$$\sum_i N_i = \rho \quad (7)$$

where W_{p02}, W_{p14}, W_{p35} are transition rates of 1050 nm pump. Signal stimulated absorption and emission are described by W_{sa} and W_{se}, respectively. The transition rates of amplified spontaneous emission at 800 nm ($^3H_4 \rightarrow {}^3H_6$) and 1800 nm ($^3F_4 \rightarrow {}^3H_6$) are governed by W_8 and W_{18} respectively. Non-radiative transition rate from $^3F_2$ to $^3F_4$ and from $^3H_5$ to $^3F_4$ are defined as A_{43}^{nr} and A_{21}^{nr}. A_{ij} is the radiative rate from level i to level j. The average concentration of thulium in the core is ρ and is quantified by [12]

$$\rho = \frac{2}{b^2}\int_0^\infty n(r) r dr$$

(8)where b is doping radius and $N(r)$ is thulium concentration profile. Interaction of the electromagnetic field with ions or transition rate (W_{ij}) can be written as [11]

$$W_{p02,p14,p35} = \lambda_{P1}\sigma_{p02,p14,p35}\left(\frac{P_{P1}^{+}}{hcA_{eff}}\right) \quad (9)$$

$$W_{8a,8e,18a,18e} = \lambda_{ASE}^{8,18}\sigma_{03,30,01,10}\left(\frac{P_{ASE}^{8,18+} + P_{ASE}^{8,18-}}{hcA_{eff}}\right) \quad (10)$$

$$W_{8a,8e,18a,18e} = \lambda_{ASE}^{8,18}\sigma_{03,30,01,10}\left(\frac{P_{ASE}^{8,18+} + P_{ASE}^{8,18-}}{hcA_{eff}}\right) + \lambda_s\sigma_{sa,se}\left(\frac{P_S^+ + P_s^-}{hcA_{eff}}\right) \quad (11)$$

where σ_{p02}, σ_{p14}, and σ_{p35} are the $^3H_6 \rightarrow {}^3H_5$, $^3F_4 \rightarrow {}^3F_2$, and $^3H_4 \rightarrow {}^1G_4$ absorption cross sections of 1050 nm forward pumping, respectively. The stimulated absorption and emission cross section of ASE at 800 and 1800 nm are denoted by σ_{8a}, σ_{8e}, and σ_{18e}, respectively. P_p^{1+} is the spectral power radiation of 1050 nm pump. P_s is the signal power and P_{ASE}, P_{ASE8}, and P_{ASE18} are the S-band ASE, 800 nm ASE and 1800 nm ASE in the forward direction (+) and backward (−) direction along the fiber. The equation to calculate W_{8a}, W_{8e}, W_{18a} and W_{18e} of single-pass TDFA are modified by integrating the reflected backward signal power P_s^- of double-pass TDFA. The lightwave propagation equations along the thulium fiber (in the z direction) can be established as follows [11,12]:

$$\frac{dP_{ASE}^{\pm}}{dz} = \pm\Gamma(\lambda_{ASE})(\sigma_{se}N_3 - \sigma_{se}N_1 + \sigma_{p01}N_0) \times P_{ASE}^{\pm} \pm \Gamma(\lambda_{ASE})2h\nu\Delta\nu\sigma_{se}N_3 \mp \alpha P_{ASE}^{\pm} \quad (12)$$

$$\frac{dP_{ASE}^{8\pm}}{dz} = \pm\Gamma(\lambda_8)(\sigma_{30}N_3 - \sigma_{03}N_1) \times P_{ASE}^{8\pm} \pm \Gamma(\lambda_8)2h\nu\Delta\nu\sigma_{30}N_3 \mp \alpha P_{ASE}^{8\pm} \quad (13)$$

$$\frac{dP_{ASE}^{18\pm}}{dz} = \pm\Gamma(\lambda_{18})(\sigma_{10}N_1 - \sigma_{01}N_0) \times P_{ASE}^{18\pm} \pm \Gamma(\lambda_{18})2h\nu\Delta\nu\sigma_{10}N_1 \mp \alpha P_{ASE}^{18\pm} \quad (14)$$

$$\frac{dP_{P1}^{+}}{dz} = -\Gamma(\lambda_{P1})(\sigma_{p02}N_0 + \sigma_{p14}N_1 + \sigma_{p02}N_3) \times P_{P1}^{+} - \alpha P_{P1}^{-} \quad (15)$$

$$\frac{dP_s^{\pm}}{dz} = \mp\Gamma(\lambda_s)(\sigma_{se}N_3 - \sigma_{sa}N_1 - \sigma_{p01}N_0) \times P_s^{\pm} \mp \alpha P_s^{\pm} \quad (16)$$

where α is background scattering loss, which is assumed to be constant for all wavelengths. λ_{ASE}, λ_{ASE8} and λ_{ASE18} are the signal wavelengths, 800 nm ASE and 1800 nm ASE, respectively. Overlapping factors between each radiation and fiber fundamental mode, $\Gamma(\lambda)$ can be expressed as [12,14]

$$\Gamma(\lambda) = 1 - e^{-(2b^2/w_0^2)} \quad (17)$$

$$W_0 = a\left(0.761 + \frac{1.237}{V^{1.5}} + \frac{1.429}{V^6}\right) \quad (18)$$

where w_0 is mode field radius defined by Eq. (18), a is core diameter, b is thulium ion dopant radius and V is normalized frequency.

3. Numerical calculations

In order to solve the population rate in steady-state condition, the time derivatives of Eqs. (1)–(6) are set to zero [15]. All the equations used for pump and signal powers, Eqs. (12)–(17), are first-order differential equations. The Runge–Kutta method is used to solve the differential equations. In the numerical modeling, we initially assume all the population to be at the ground level ($^3H_6$). Table 1 shows the initial conditions, which are set on pump power, signal power and ASE spectrum at S-band, 800 and 1800 nm wavelength [16]:

Table 1. Initial condition.

Initial condition	Operating wavelength	Explanation
$P_{P1}(z=0) = P_{P1}$	$\lambda = 1050$	Initial condition for 1050 nm pump at $Z = 0$
$P_S(z=0) = P_S$	–	Initial condition for signal pump at $Z = 0$
$P_{ASE}^{+}(z=0,v) = P_{ASE}^{-}(z=l,v) = 0$	$1460 < \lambda < 1050$	Initial condition for $P_{ASE}^{\pm}$ at s-band for $Z = 0$ and $Z = L$
$P_{ASE}^{8+}(z=0,v) = P_{ASE}^{8-}(z=l,v) = 0$	$1460 < \lambda < 1050$	Initial condition for $P_{ASE}^{\pm}$ at 800 nm for $Z = 0$ and $Z = L$
$P_{ASE}^{18+}(z=0,v) = P_{ASE}^{18-}(z=l,v) = 0$	$1460 < \lambda < 1050$	Initial condition for $P_{ASE}^{\pm}$ at 1800 nm for $Z = 0$ and $Z = L$

The thulium-doped fiber with length L is divided into L segments along the z direction, as shown in Fig. 3. We solve for the pump, signal and ASE power propagating in the first segment (segment 0) by using the above initial conditions. For the following segments (segment 1–L−1), the power for all the pump, signal and ASE at one end of a segment is used as the input for the next segment [17]. Relaxation method is used to achieve an accuracy of 0.01% for all the pump, signal and ASE powers [16].

The spectroscopic parameters used in our analysis are carefully chosen from the literature [6,11,18] and are summarized in Table 2. The spectral emission cross section at S-band of thulium ion [8] and the spectral absorption cross section at S-band can be estimated by the modified McCumber's relation [14]:

$$\sigma_a(v) = \frac{\sigma_e(v)}{\eta^{peak}} \exp\left(\left\{\frac{h(v - v^{peak})}{k_B T}\right\}\right) \quad (21)$$

Fig. 3. Schematic of the fiber model.

$$\eta^{peak} = \frac{\sigma_e^{peak}}{\sigma_a^{peak}}. \quad (22)$$

where k_B is the Boltzmann constant and T is temperature. As observed experimentally, the absorption cross section peak is approximately 70% of the emission peak [6]. Fig. 4 shows the emission cross section spectrum and

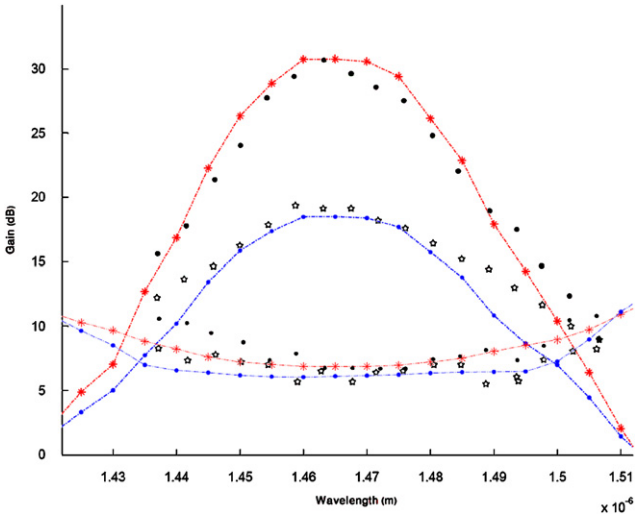

Fig. 4. Gain and noise figure characteristics for both single-pass and double-pass TDFAs.

Table 2. Parameter used in the numerical simulation.

Parameter	Unit	Symbol	Value
Thulium concentration	$1/m^3$	ρ	1.68×10^{25}
Numerical aperture		NA	0.3
Fiber length	m	L	20
Background lost	dB/m	α	1.68×10^{25}
Effective area	m^2	A_{eff}	2.096×10^{-12}
Division along fiber			12
800 nm ASE bandwidth	nm	Δv_8	10
1800 nm ASE bandwidth	nm	Δv_{18}	100
ASE bandwidth	nm	Δv	2
1050 nm Pump absorption cross section			
Section	m^2	σ_{p02}	1.1×10^{-27}
1050 nm Pump absorption cross section	m^2	σ_{p14}	8.2×10^{-25}
1050 nm Pump absorption cross section	m^2	σ_{p35}	2.5×10^{-27}
1650 nm Pump absorption cross section	m^2	σ_{p01}	2×10^{-26}
Signal absorption cross section	m^2	σ_{sa}	Fig
Signal stimulated emission cross section	m^2	σ_{se}	Fig
800 nm transition cross section	m^2	σ_{03}, σ_{30}	6.2×10^{-25}
1800 nm transition cross section	m^2	σ_{01}, σ_{10}	5.2×10^{-25}
Radiative decay rate	1/s	A_{10}	172.4
Radiative decay rate	1/s	A_{30}	702.8
Radiative decay rate	1/s	A_{50}	676.3
Radiative decay rate	1/s	A_{52}	492.9
Non-radiative decay rate	1/s	A_{43}^{nr}	52976
Non-radiative decay rate	1/s	A_{21}^{nr}	165626

the absorption cross section spectrum from Eq. (21) of the thulium-doped fiber in fluoride host.

4. Results and discussion

The model is numerically resolved using a Runge–Kutta method. Here we first compare the gain and noise figure characteristics between the single-pass and double-pass TDFA as shown in Fig. 4. For comparison, the 1050 nm pump and input signal powers are set at 250 mW and −30 dBm, respectively. As shown in the figure, the gain is higher in a double-pass amplifier compared to the single-pass amplifier. The double-pass amplifier achieves a maximum gain of 32 dB at 1465 nm, which is 15 dB higher than the single-pass TDFA. The gain enhancement is attributed to the longer effective length in the double-pass TDFA. With the double-pass configuration, the effective TDF amplification length is twice the TDF length of the single-pass configuration, where the signals make one round-trip in the fiber. Therefore, the gain is higher in the double-pass amplifier. However, the noise figure is higher in the double-pass amplifier compared to the single-pass as shown in Fig. 5. For instance, a 1 dB of noise figure penalty is observed at 1470 nm in the double-pass amplifier compared with the single-pass amplifier. This increase in the noise figure is due to the counter-propagating ASE at the input part of the TDFA, which reduces the population inversion at the input part of the fiber and subsequently increases the noise figure [19]. As shown in Fig. 4 we compare our result with experimental work of J.A. Camrlo in 2003 that represent the double-pass single pump 1050 nm pump power with the same setup [20]. The theoretical gain and noise figure is in agreement with the experimental results.

Figs. 5 and 6 show the gain and noise figures of the double-pass TDFA, respectively, with variations of 1050 nm pump power from 0 to 300 mW and variations of input signal power from −40 to 0 dBm. The TDF length and input signal wavelength is set at 20 m and 1460 nm, respectively. As shown in Fig. 6, the gain gradually decreases with the increment of input signal power. This is due to the pump being unable to replenish the inversion as fast as the input signal is depleting it. The gain also increases with pump power and finally saturates at a certain pump power. The saturation pump power reduces with the increase of input signal power as shown in Fig. 6. The maximum gain of 42 dB is obtained at an input signal power of −40 dBm with a pump power of 300 mW. The noise figure can be reduced (improved) by either increasing the pump power or reducing the input signal power as shown in Fig. 6. The noise figure at a particular wavelength is calculated by the equation $NF = 1/G + P_{ASE}/(G \times h \times \nu \times \Delta\nu)$ where G and P_{ASE} is gain and ASE power, respectively. This equation shows that the noise figure reduces as the gain increases which is in agreement with our results.

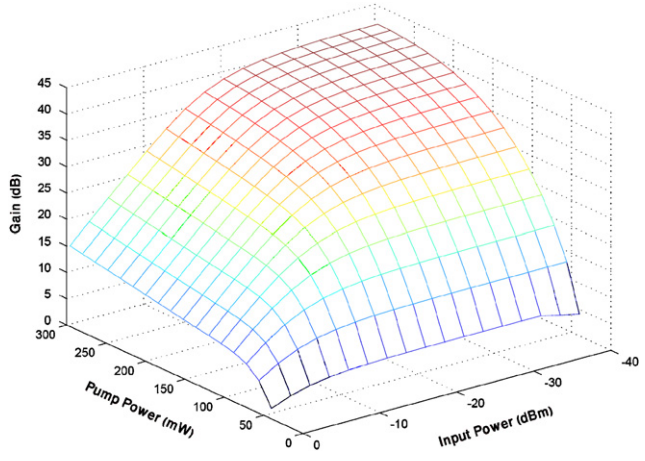

Fig. 5. Gain vs pump power and input signal power for the double-pass TDFA.

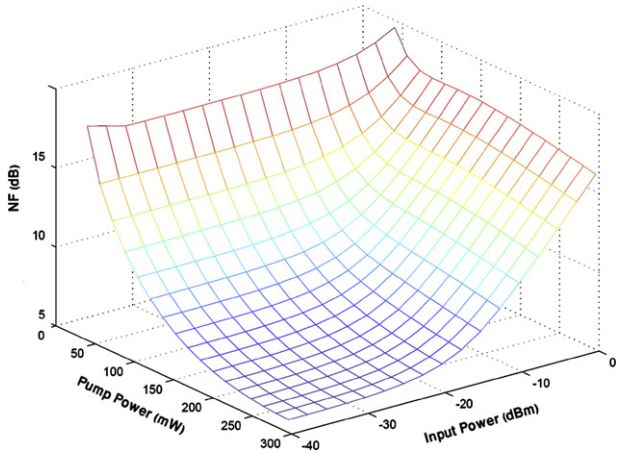

Fig. 6. Noise figure vs pump power and input signal power for the double-pass TDFA.

5. Conclusion

In this paper an efficient fluoride-based thulium-doped fiber amplifier (TDFA) in a double-pass configuration is demonstrated theoretically. The double-pass TDFA incorporates a reflector to allow double propagation of the test signal in the thulium gain medium and thus improves the TDFA gain. The theoretical analysis uses the Runge–Kutta method to solve the differential equations. The proposed TDFA shows a small signal gain improvement of more than 15 dB in the 1465 nm region, with a gain as high as 42 dB obtained in this region at a 1050 nm pump power of 300 mW and a 20 m of thulium-doped fiber. However, a noise figure penalty of about 1 dB is also obtained at this wavelength region

compared to a single-pass configuration, due to the reduction in the population inversion by the counter-propagating ASE. The theoretical results are in agreement with the experimental results.

References

[1] R. Caspary, U.B. Unrau, W. Kowalsky, Recent progress on "S-band fiber amplifiers," in: Proceedings of 2003 5th International Conference on Transparent Optical Networks, vol. 1, 2003, pp. 236–242.

[2] T. Sakamoto, S-band fiber optic amplifiers, Conference and Exhibition on Optical Fiber Communication OFC, vol. 2, 2001, pp. TuQ1-1–TuQ1-4.

[3] M.M. Kozak, R. Caspary, W. Kowalsky Thulium-doped fiber amplifier for the S-band, in: Proceedings of 2004 6th International Conference on Transparent Optical Networks, vol. 6, 2004, pp. 51–54.

[4] F. Roy, F. Leplingard, L. Lorcy, A. Le Sauze, P. Baniel, D. Bayart, 48% power conversion efficiency in single pump gain-shifted thulium-doped fibre amplifier, Electron. Lett. 37 (15) (2001) 943–945.

[5] T. Kasamatsu, Y. Yano, H. Sekita, 1.50-mm-band gain-shifted thulium-doped fiber amplifier with 1.05- and 1.56-mm dual-wavelength pumping, Opt. Lett. 24 (23) (1999) 1684–1686.

[6] T. Kasamatu, Y. Yano, T. Ono, 0.49 μm band gain-shifted thulium doped fiber amplifier for WDM transmission system, J. Lightwave Technol. 20 (10) (1998) 1826.

[7] R. Caspary, M.M. Kozak, and W. Kowalsky, Avalanche pumping of thulium doped S-band fiber amplifiers, International Conference on Transparent Optical Networks, vol. 1, 2006, pp. 166–169.

[8] R. Allen, L. Esterowitz, I. Aggarwal, An efficient 1.46 μm thulium fiber laser via a cascade process, IEEE J. Quantum Electron. 29 (2) (1993) 303–306.

[9] J.F. Martins-Filho, C.J.A. Bastos-Filho, M.T. Carvalho, M.L. Sundheimer, A.S.L. Gomes, Dual-wavelength (1050 nm + 1550 nm) pumped thulium-doped fiber amplifier characterization by optical frequency-domain reflectometry, Photonics Technol. Lett. 15 (1) (2003) 24–26.

[10] C.J.A. Basto-Filho, J.F. Martins-filho, A.S.L. Gomes, 38 dB Gain from double-pass single-pump thulium doped fiber amplifier, IEEE Microwave and Optoelectronics Conference, vol. 1, 2003, pp. 125–128.

[11] S.S.H. Yam, J. Kim, Ground state absorption in thulium-doped fiber amplifier: experiment and modeling, IEEE J. Select. Top. Quantum Electron. 12 (4) (2006) 797–803.

[12] P. Peterka, B. Faure, W. Blance, M. Karasek, Theoretical modeling of S-band thulium doped silica fiber amplifiers, Opt. Quantum Electron. 36 (2004) 201–212.

[13] T. Komukai, T. Yamamoto, T. Sugawa, Y. Miyajima, Upconversion pumped thulium-doped fluoride fiber amplifier and laser operating at 1.47 μm, J. Quantum Electron. 31 (11) (1995) 1880–1889.

[14] E. Desurvire, Erbium-doped Fiber Amplifiers: Principles and Applications, Wiley, New York, 1994.

[15] W.J. Lee, B. Min, J. Park, N. Park, Study on the pumping wavelength dependency of S/S + -band fluoride based thulium doped fiber amplifiers, Optical Fiber Communication Conference and Exhibit, OFC, vol. 2, 2001, pp. TuQ5-1–TuQ5-4.

[16] M. Karasek, Optimum design of Er3 + /Yb3 + Co-doped fibers for large signal high-pump-power applications, IEEE J. Quantum Electron. 33 (10) (1997) 1699–1705.

[17] M. Eichhorn, Numerical modeling of Tm-doped double-clad fluoride fiber amplifiers, IEEE J. Quantum Electron. 41 (12) (2005) 1574–1581.

[18] J. Michael, F. Digonnet, Rare-earth-doped Fiber Lasers and Amplifiers, CRC Press, Boca Raton, FL, 2001.

[19] S.W. Harun, N.K. Saat, H. Ahmad, An efficient S-band Erbium-doped fiber amplifier using double-pass configuration, IEICE Electron. Express 2 (6) (2005) 182–185.

[20] C.J.A. Martins-Filho, J.F. Martins-Filho, A.S.L. Gomes, 38 dB Gain from double pass single pump thulium doped fiber amplifier, IEEE Microwave and Optoelectronics Conference, vol. 1, 2003, pp. 125–128.